Plant Physiology®

Plant Physiology, 2026, **200**, kiaf648
https://doi.org/10.1093/plphys/kiaf648
Advance access publication 12 December 2025
Research article

Mitochondria affect photosynthesis through altered tissue levels of O_2

Matleena Punkkinen,[1] Bikash Baral,[1] Olga Blokhina,[1,†] Lucas León Peralta Ogorek,[2,3,†] Minsoo Kim,[4,7,†] Kurt Fagerstedt,[1] Mikael Brosché,[1] Lauri Nikkanen,[5] Elizabeth Vierling,[4] Ole Pedersen,[2] and Alexey Shapiguzov[1,6,*]

[1]Organismal and Evolutionary Biology (OEB), Viikki Plant Science Centre (ViPS), Faculty of Biological and Environmental Sciences, University of Helsinki, Helsinki 00014, Finland
[2]Freshwater Biological Laboratory, Department of Biology, University of Copenhagen, Copenhagen 2100, Denmark
[3]School of Biosciences, University of Nottingham, Sutton Bonington LE12 5RD, United Kingdom
[4]Department of Biochemistry & Molecular Biology, University of Massachusetts Amherst, Amherst, MA 01003, United States
[5]Molecular Plant Biology, Department of Life Technologies, University of Turku, Turku 20014, Finland
[6]Natural Resources Institute Finland (Luke), Production Systems, Turku 20800, Finland
[7]Present address: Howard Hughes Medical Institute and Department of Molecular Biology, Massachusetts General Hospital, Boston MA 02114, United States.
*Author for correspondence: alexey.shapiguzov@helsinki.fi (A.S.)
[†]These authors contributed equally to the manuscript.
The author responsible for distribution of materials integral to the findings presented in this article in accordance with the policy described in the Instructions for Authors (https://academic.oup.com/plphys/pages/General-Instructions) is Alexey Shapiguzov (alexey.shapiguzov@helsinki.fi).

Abstract

Oxygen (O_2) availability in plant tissues is dynamically shaped by photosynthesis and respiration and is linked to stress responses and development. While mitochondria are the primary consumers of cellular O_2, their impact on chloroplast functions under low-oxygen conditions remains insufficiently understood. Mitochondrial retrograde signaling activates expression of nuclear genes encoding alternative oxidases and other respiratory components, and high abundance of these enzymes coincides not only with changes in respiration but also with alterations in chloroplast functions. For example, plants with induced mitochondrial signaling are tolerant to methyl viologen, which catalyzes the chloroplastic Mehler reaction. The mechanism of this inter-organelle interaction remains unclear. Here, we investigated respiration, photosynthesis, and in vivo O_2 levels in Arabidopsis (*Arabidopsis thaliana*) mutants and transgenic lines with perturbations in diverse mitochondrial functions, including defects in respiratory complex I, ATP synthase, mitochondrial protein processing, transcription, nucleoid organization, and organelle architecture, as well as in lines with altered mitochondrial signaling, alternative oxidase activities, and nitric oxide metabolism. Increased abundance and capacity of alternative oxidases correlated with elevated O_2 consumption in darkness, slower O_2 re-accumulation in light, and reduced effects of methyl viologen on chloroplasts. The changes are likely mediated by multiple stress-induced alternative respiratory components. Our results support the hypothesis that enhanced mitochondrial O_2 consumption under stress lowers tissue O_2 levels, thereby modifying chloroplastic electron transfer and ROS metabolism. These data provide insights into the establishment and sensing of hypoxia in plants, plant adaptation to mitochondrial stress and low-oxygen environments, and the roles of chloroplasts in these processes.

Introduction

Cellular consumption, production, and sensing of molecular oxygen (O_2) are tightly integrated with plant metabolic and signaling networks (Bailey-Serres et al. 2024; Renziehausen et al. 2024; Van Veen et al. 2024). Oxygen availability in plant tissues fluctuates over diurnal cycles, influenced by both photosynthesis and respiration (Triozzi et al. 2024). Localized hypoxia, which can be caused by elevated mitochondrial respiration, has been implicated in stress acclimation (Wang et al. 2020) and developmental regulation (Weits et al. 2021; Iida et al. 2025). These observations highlight a link between low-oxygen signaling and energy metabolism.

Mitochondria are the main consumers of cellular O_2. In these organelles, O_2 acts as the terminal electron acceptor for respiration in the cytochrome *c* oxidase (COX) and alternative oxidase (AOX) pathways. AOXs, together with alternative NAD(P)H dehydrogenases (NDs), form a stress-inducible, non-phosphorylating electron transfer system that dissipates excessive reducing power (Yoshida and Noguchi 2011; Vanlerberghe 2013; Wagner et al. 2018 ; Shameer et al. 2019; Møller et al. 2021). The alternative respiratory pathway is often induced under stress and is associated with mitochondrial retrograde signaling, which activates a set of nuclear genes referred to as the mitochondrial dysfunction stimulon (MDS) (De Clercq et al. 2013; Ng et al. 2013; Shapiguzov et al. 2019; Eysholdt-Derzsó et al. 2023; Khan et al. 2024). MDS signaling plays an important role in the adaptation of plants to low-oxygen levels (Renziehausen et al. 2024).

While the roles of mitochondria under changing tissue O_2 levels are well established, how chloroplast functions integrate into this network remains less clear. Inside the chloroplast, O_2 is produced by light-driven water splitting and consumed by photorespiration (Bauwe et al. 2010), the plastid terminal oxidase (PTOX) (Nawrocki et al. 2015), and the Mehler reaction (Miyake 2010). In the Mehler reaction, electrons are transferred from photosystem I (PSI) to O_2, generating reactive oxygen species (ROS). Interestingly, ROS metabolism of the chloroplast is sensitive to mitochondrial MDS signaling: plants with activated MDS exhibit

Received: September 5, 2025. Accepted: October 29, 2025.

tolerance to methyl viologen (MV, also known as paraquat) (De Clercq et al. 2013; Ng et al. 2013; Shapiguzov et al. 2019), a catalyst of the Mehler reaction. Treatment with MV generates ROS that can overwhelm the chloroplast antioxidant systems, resulting in photoinhibition and cell death (Farrington et al. 1973 ; Nishiyama et al. 2011; Shapiguzov et al. 2019). Another phenotype associated with MDS activation is a more reduced redox state of chloroplast thiol enzymes (Shapiguzov et al. 2019 , 2020). This is consistent with attenuation of the Mehler reaction, as Mehler-derived ROS are the main oxidants of these enzymes (Ojeda et al. 2018; Vaseghi et al. 2018; Yoshida et al. 2018).

We previously proposed that elevated mitochondrial respiration in plants with active MDS reduces O_2 availability, thereby modifying ROS metabolism of the chloroplast (Shapiguzov et al. 2020). However, direct evidence for altered O_2 levels has been lacking. In this study, we investigated photosynthesis, respiration, and in vivo O_2 levels in a set of Arabidopsis (*Arabidopsis thaliana*) mutants and transgenic lines with defects in diverse mitochondrial functions (Fig. 1), including respiratory complex I (*ndufa1*, *ndufs4*, *rug3*), ATP synthase (*ATPd* RNAi line here called *ATPQi*), protein processing (*phb3*, *lon1*), transcription and nucleoid organization (*rpoTmp*, *shot1*, *atad3a1 atad3b1*:*ATAD3A1-GFP* here called *ATAD3A1-GFP*), and architecture and fission (*drp3a drp3b*, *mic60*). Additionally, we examined mutants and transgenic lines with altered MDS signaling and AOX activities (*rcd1*, *rcd1 anac017*, *ANAC013* overexpressor line *ANAC013*-OE, *aox1a*, *aox1a aox1d*, *AOX1a* overexpressor line here called *AOX1a*-OE), or altered nitric oxide (NO) metabolism (*hot5* and a *GSNOR* overexpressor line *GSNOR-GFP*).

Our results support the hypothesis that enhanced mitochondrial O_2 consumption under stress conditions contributes to lower tissue levels of O_2, which in turn affects chloroplast functions and photosynthesis. These data provide insights into the establishment and sensing of hypoxia in plants, plant adaptation to mitochondrial stress and low-oxygen environments, and the roles of chloroplasts in these processes.

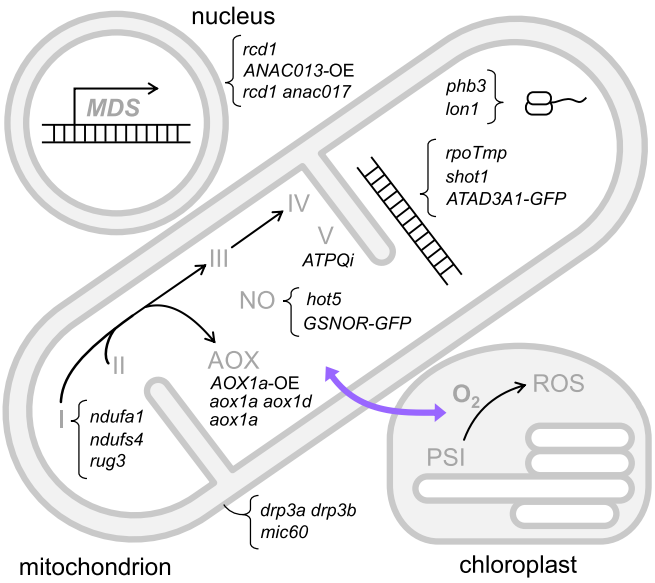

Figure 1. Diagram of mutants and transgenic lines used in the study. We utilized a set of mutants and transgenic lines with a wide variety of mitochondrial perturbations to examine the interactions between mitochondrial respiration and the chloroplastic Mehler reaction (purple arrow). The mutants and transgenic lines are written in italics next to the affected functions, pathways, or complexes. References for all lines are provided in Materials and methods.

Results

Mitochondrial perturbations modify plants' responses to MV

Mitochondrial defects associated with increased MDS signaling coincide with changes in the chloroplasts (De Clercq et al. 2013; Ng et al. 2013; Shapiguzov et al. 2019, 2020). To test whether this is a general response to various mitochondrial perturbations, rather than a consequence of specific mitochondrial defects, we studied reactions to MV in a set of Arabidopsis mutants and transgenic lines with impaired mitochondrial functions (Fig. 1). We began by assessing the tolerance of these lines to MV-induced photoinhibition, an indication of damage to photosynthetic apparatus due to ROS. Leaf discs were floated overnight in darkness on solutions with or without MV to facilitate uptake of the chemical. After incubation, MV toxicity was induced by 15 repeated 1-h light periods (450 nm, 80 µmol m^{-2} s^{-1}) each followed by a 20-min dark acclimation period and a measurement of maximal quantum yield of photosystem II (PSII) (Fv/Fm). No significant changes were observed in either Fv/Fm or leaf AOX abundance during the overnight incubation of leaf discs (Supplementary Figure S1a and b). After the overnight incubation but before the start of the light exposure, Fv/Fm was in the range of 0.8 to 0.85 in both MV-treated and control samples of all tested genotypes (Supplementary Figure S1c). This indicated that the assessed effects of MV were light-dependent and thus likely caused by MV action in the chloroplast. Several plant lines that are affected in different mitochondrial processes were more tolerant to MV, maintaining relatively stable Fv/Fm values during 15 h of light treatment, in comparison to the wild type (Col-0) that showed a dramatic reduction in PSII quantum yield (Fig. 2a). A comparison of end point Fv/Fm values for all lines (Fig. 2b) shows that over half of the tested genotypes that are deficient in diverse mitochondrial functions exhibit resistance to chloroplastic ROS stress.

In addition to its long-term effects on chloroplasts and the photosynthetic apparatus associated with ROS production, MV also induces rapid changes in the redox state of the photosynthetic electron transfer chain. These changes are detectable already within one second of light exposure (Shapiguzov et al. 2020). The effect is likely caused by MV acting as a strong electron sink at the electron-acceptor side of PSI, withdrawing electrons from the FeS clusters (Tiwari et al. 2024). This promotes oxidation of the photosynthetic electron transfer chain and thus faster quenching of chlorophyll fluorescence. We previously showed that in a normoxic atmosphere (normal air), the quenching effect that MV has on chlorophyll fluorescence is indistinguishable between the wild type and *rcd1*. However, under hypoxia, MV-induced chlorophyll fluorescence quenching diminished in *rcd1* while remaining high in the wild type (Shapiguzov et al. 2020). We therefore tested the effects of MV under a hypoxic atmosphere in all lines. We floated leaf discs overnight on solutions with or without MV in darkness under ambient atmosphere. Next, we introduced a hypoxic environment by flushing nitrogen gas over the leaf discs for 20 min in darkness, and finally, we performed light treatments and recorded the chlorophyll fluorescence responses.

First, we measured the rapid (within 50 s) dark relaxation of maximal chlorophyll fluorescence (Fm) triggered by a saturating light pulse (Fig. 2c and d), then the dynamics of chlorophyll fluorescence under low-intensity actinic light (Fig. 2e and f). In both types of measurements, chlorophyll fluorescence responses were similar

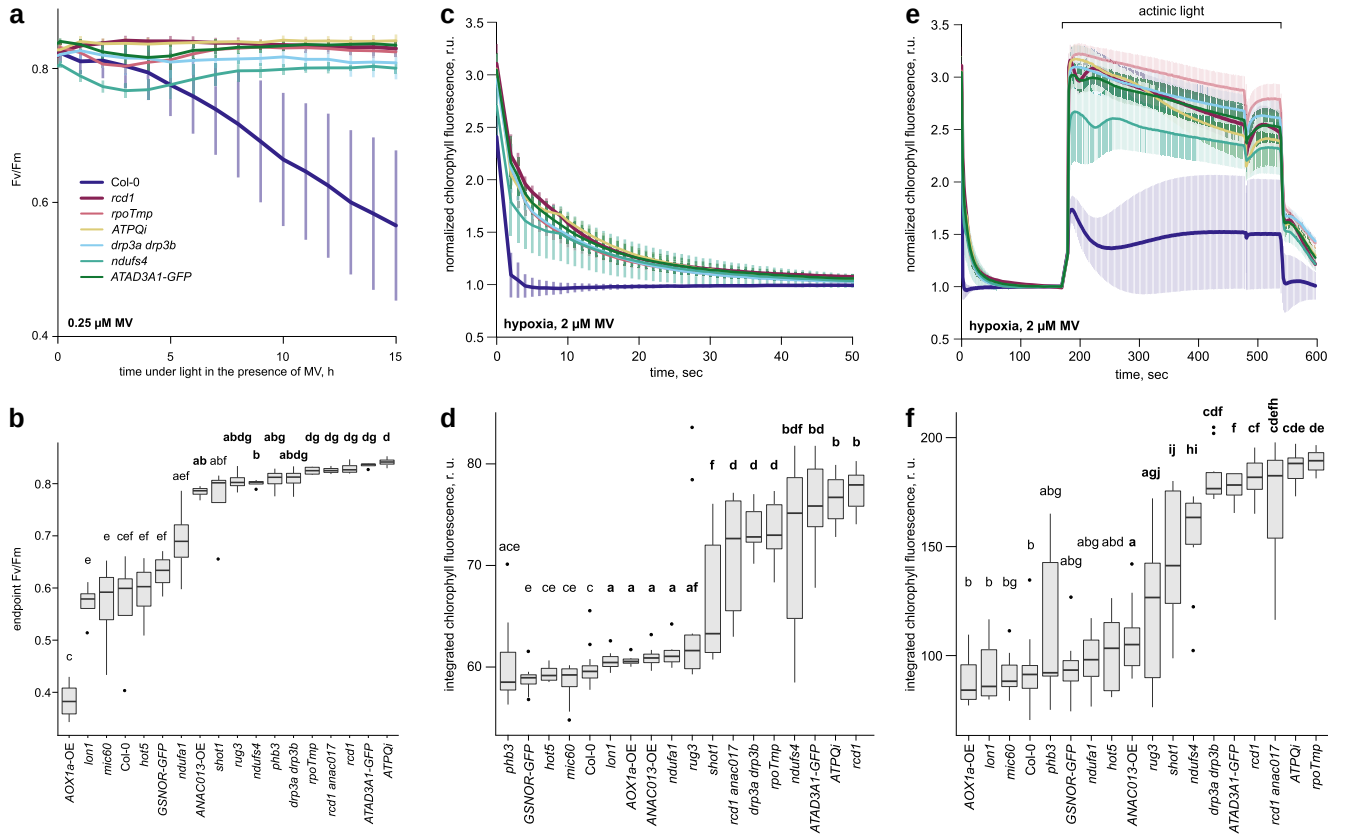

Figure 2. MV-induced responses in plant lines with perturbed mitochondrial functions. a and b) MV-induced photoinhibition. Repeated exposure of MV-treated leaf discs to light led to a gradual decline of maximal PSII quantum yield (Fv/Fm) in susceptible genotypes such as Col-0, while other lines retained PSII function. The kinetics of Fv/Fm in selected MV-tolerant lines compared to wild type during long-term illumination are shown in a) as averages (±SD) measured from at least 4 individual plants. Fv/Fm values for all tested lines at the 15 h time point are shown in b), with box plots indicating the median (horizontal line), first and third quartiles (box), and minimum and maximum (whiskers) arranged in order of increasing mean. Statistically significant groups (Kruskal–Wallis test, $P < 0.05$) are indicated with letters, bolded for plant lines that have higher Fv/Fm than the wild type. c to f) MV-induced quenching of chlorophyll fluorescence under hypoxia. Several plant lines displayed resistance to MV-induced chlorophyll fluorescence decay under hypoxic atmosphere, in contrast to MV-sensitive lines such as Col-0. This was observed both in dark relaxation of Fm c, d) and in light-adapted fluorescence under actinic light e, f). Values shown in c, e) are averages (±SD), the box plots d, f) indicate the median (horizontal line), first and third quartiles (box), minimum and maximum (whiskers) measured from at least 5 individual plants. Kinetics of chlorophyll fluorescence in selected lines are shown in c) and e); image c) is a magnified view of the first 50 s of e). Fluorescence responses were quantified by calculating the integrated area under the curve for dark relaxation of Fm d) and light-adapted fluorescence f), with genotypes arranged in order of increasing mean. Statistically significant groups are indicated with letters; bolded letters indicate lines with higher remaining chlorophyll fluorescence than the wild type (Kruskal–Wallis test, $P < 0.05$). Both sets of experiments were repeated twice with similar results. MV, methyl viologen.

in all lines under a normoxic environment (Supplementary Figure S2a and b and Supplementary Dataset S1) and under hypoxic atmosphere without MV (Supplementary Figure S2c and Supplementary Dataset S1). However, under hypoxic conditions, the effect of MV on fluorescence quenching was strikingly different between the genotypes (Fig. 2c to f; Supplementary Dataset S1). In wild-type plants, MV still efficiently quenched chlorophyll fluorescence, while in several lines with impaired mitochondria, fluorescence dynamics of MV-treated samples became indistinguishable from untreated controls (compare Fig. 2e and Supplementary Figure S2c). These results indicate that O_2 availability is crucial for mitochondrial modulation of the measured chloroplast functions.

The main known pathways through which O_2 affects chloroplastic electron flows are the Mehler reaction at the PSI acceptor side, the activity of the chloroplast terminal oxidase PTOX, and photorespiration. PTOX was previously not implicated in MV tolerance (Shapiguzov et al. 2019). To test whether the observed toxicity of MV is linked to photorespiration, we first studied the responses of several plant lines to MV-induced photoinhibition under elevated CO_2 concentration (~1,000 ppm), which suppresses photorespiration, versus normal atmospheric CO_2 (450 ppm). The Fv/Fm dynamics were very similar under both conditions in the studied lines (Supplementary Figure S3). Next, we performed MV-induced photoinhibition analyses in mutants deficient in photorespiration: *cat2* (lacking peroxisomal CATALASE 2), *gox1* (lacking GLYCOLATE OXIDASE 1), *cat2 gox1*, and *rcd1 cat2*. Of these mutants, *cat2*, *gox1*, and *cat2 gox1* responded to MV in a similar manner to wild type, while *rcd1 cat2* performed similarly to *rcd1* (Supplementary Figure S4). These results indicate that photorespiration does not substantially contribute to the observed interaction between the organelles, thereby narrowing our focus to the Mehler reaction.

The above experiments showed that various mitochondrial perturbations suppressed the effects of MV on chloroplasts, indicating altered ROS metabolism and photosynthetic electron transfer, and that this organelle interaction is sensitive to O_2 availability.

Mitochondria influence the Mehler reaction at PSI in an oxygen-dependent manner

To probe the activity of MV at its site of action on the electron-acceptor side of PSI, we measured the oxidation state

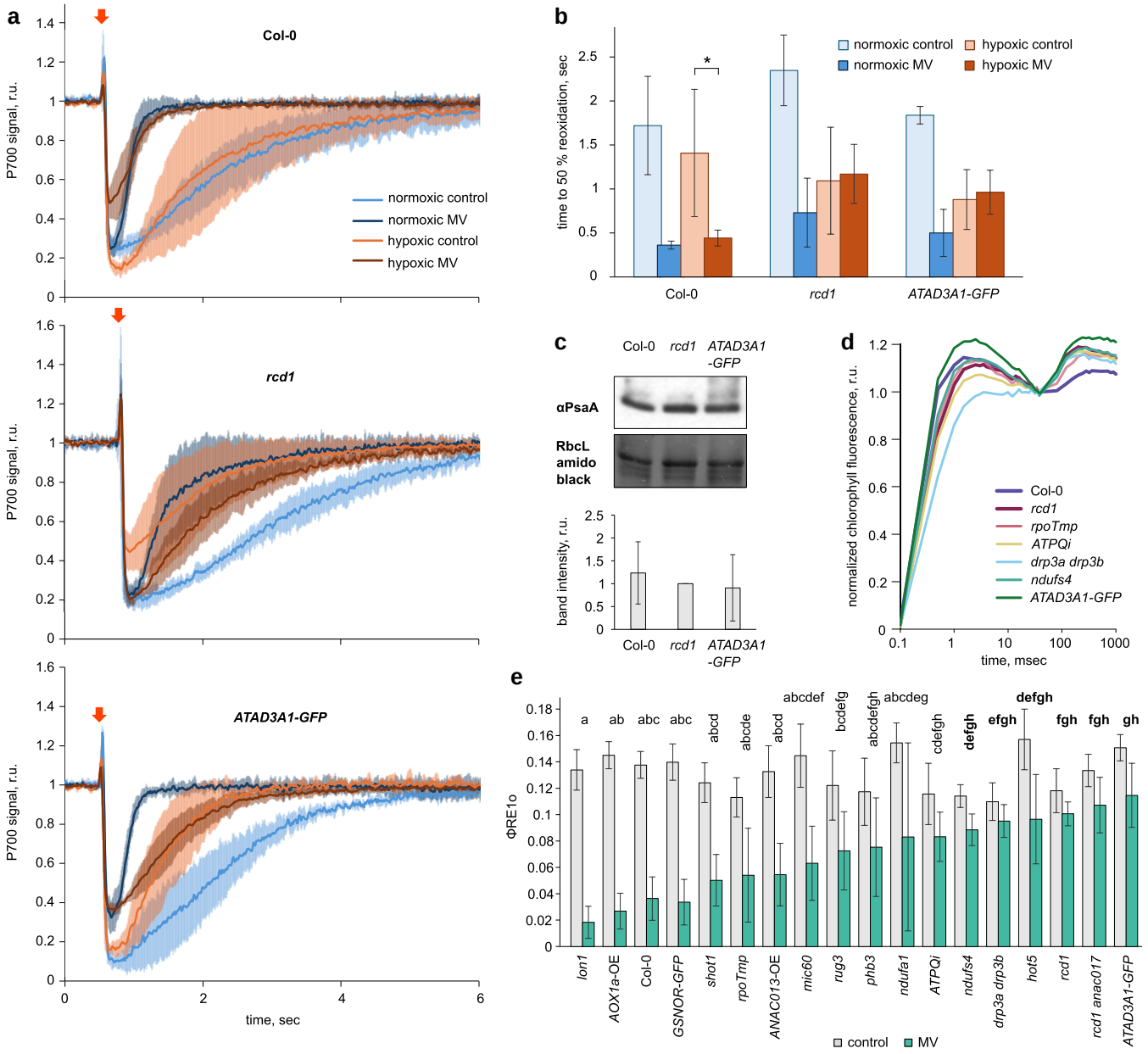

Figure 3. PSI oxidation in the presence of MV under hypoxic conditions in plant lines with perturbed mitochondrial functions. P700 reoxidation kinetics after a saturating flash of red (PSII-specific) light (red arrow) over the far-red (PSI-specific) background in leaves pretreated with MV or untreated are shown in a). P700 dynamics were quantified by measuring the time required to reach 50% of the initial P700 oxidation level after the red flash b). Statistically significant difference between hypoxic results (Mann–Whitney *U* test, $P < 0.05$) is indicated with an asterisk. Values are averages (±SD) from at least 4 individual plants. No statistically significant differences were detected in PSI abundance in total leaf extracts assessed by immunoblotting with an αPsaA antibody. Values are averages (±SD) from at least 4 individual plants. The PsaA signal was normalized to *rcd1* c). OJIP kinetics were determined to examine the effects of MV directly on the electron-acceptor side of PSI. Kinetics in selected lines under hypoxic conditions in leaf discs treated with 2 μM MV are shown in d). Quantification of ϕRE1o was used as an indicator of the I-P rise, corresponding to PSI activity e). Values are averages (±SD) from at least 4 individual plants with genotypes arranged in the order of increasing mean under MV. Statistically significant groups are indicated with letters, bolded for lines that have higher ϕRE1o value in the presence of MV than wild type (Kruskal–Wallis test, $P < 0.05$). The experiment was performed 3 times with similar results. MV, methyl viologen.

of PSI reaction center P700 using DUAL-PAM. Detached leaves were pretreated with 1 μM MV and placed in transparent bags with or without an AnaeroGen anaerobic gas generator, after which light treatments and spectroscopic measurements were performed through the plastic. Far red light (720 nm), preferentially absorbed by PSI, was turned on to oxidize P700. Next, a saturating red light flash (635 nm), preferentially absorbed by PSII, was turned on to transiently reduce P700 in the far red light background. As expected, the reoxidation rate of P700 was strongly enhanced by MV in normoxic controls (Fig. 3a). In leaves under hypoxic conditions, MV still accelerated PSI oxidation in Col-0, but not in *rcd1* or *ATAD3A1-GFP* (Fig. 3a and b). Importantly, immunoblotting of these lines with the αPsaA antibody revealed no difference in PSI abundance (Fig. 3c).

As a complementary approach, we performed flash-induced chlorophyll fluorescence imaging, similarly to the measurements in Shapiguzov et al. (2020). The polyphasic rise of chlorophyll fluorescence triggered by a saturating light pulse, the OJIP transient,

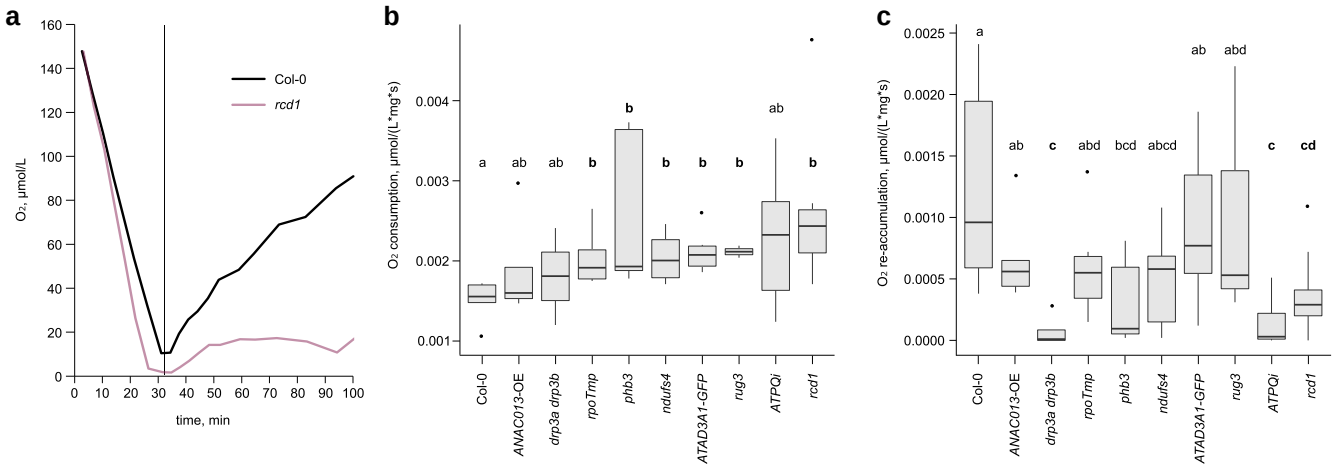

Figure 4. O_2 consumption and accumulation dynamics in plant lines with perturbed mitochondrial functions. O_2 dynamics in selected plant lines were examined by measuring O_2 fluctuations in cuvettes where aerial parts of plate-grown plants were immersed in analysis buffer. An example of this assay performed with Col-0 and *rcd1* is shown in a), with relative O_2 consumption rate first recorded in darkness. After O_2 concentrations approached 0, the light was turned on (vertical line at approx. 30 min) and O_2 re-accumulation caused by photosynthetic O_2 evolution was recorded. Consumption b) and re-accumulation c) rates of O_2 were obtained from the kinetics as shown in a). The box plots indicate the median (horizontal line), first and third quartiles (box), minimum and maximum (whiskers) measured in at least 3 replicates, with each replicate consisting of several individual seedling aerial parts. The genotypes are arranged in order of increasing mean in b), and in c), they are in the same order as in b). Statistically significant groups are indicated with letters, which are bolded for lines that have higher O_2 consumption or lower O_2 re-accumulation rates than wild type (Kruskal–Wallis test, $P < 0.05$).

reflects electron transfer dynamics through different parts of the photosynthetic electron transfer chain. The O-J phase corresponds to PSII, the J-I phase to the intersystem electron transfer chain, and the I-P rise to PSI activity (Strasser et al. 2004; Stirbet and Govindjee 2011, 2012; Schreiber and Klughammer 2021; Schreiber 2023). MV application specifically diminished the I-P rise, indicating oxidation of PSI in all tested lines (Supplementary Figure S5). However, following 60 min of nitrogen flushing in darkness to induce hypoxia, the extent of the I-P rise varied among the lines (Fig. 3d). We calculated $\phi RE1o = 1 - Fi/Fm$, a parameter sensitive to MV effects on the I-P rise (Strasser et al. 2004; Shapiguzov et al. 2020), for MV-treated samples and their controls. MV continued to suppress the I-P rise in the wild type, but its effect was significantly diminished in several lines with impaired mitochondria (Fig. 3e; Supplementary Dataset S1).

Together, these analyses demonstrated that the redox effects of MV on photosynthetic electron transfer, and specifically on PSI, are modified in lines with altered mitochondrial functions. Notably, these differences only became apparent under hypoxic conditions. This suggests that the interaction between altered mitochondrial functions and PSI is dependent on O_2 availability.

Mitochondrial defects modify O_2 consumption and accumulation rates in vivo

Observing that the effects of MV on chloroplasts were modulated by an externally generated hypoxic atmosphere prompted us to study whether altered responses of mitochondrial mutants to MV were linked to tissue O_2 levels. We hypothesized that the changes in respiration caused by mitochondrial defects could affect tissue O_2 availability, thereby modulating the effects of MV. Thus, we selected a subset of lines with the strongest changes in MV response compared to the wild type and measured their rates of O_2 consumption in darkness and O_2 re-accumulation in light. An example of such an assay is shown in Fig. 4a. We found several lines that had higher O_2 consumption rates in darkness or lower O_2 re-accumulation rates in light than in the wild type (Fig. 4b and c). Since studies in *rcd1* showed no defects in the chloroplast proteome (Shapiguzov et al. 2019) or O_2 evolution (Shapiguzov et al. 2020), the changes in O_2 re-accumulation rate were likely due to increased reuptake of photosynthetically evolved O_2 instead of decreased O_2 evolution.

Next, we performed a similar experiment in the presence of the AOX inhibitor salicylhydroxamic acid (SHAM). SHAM reduced the above differences between the lines (Supplementary Figure S6), which suggests that the differences in O_2 dynamics could be related to different levels of AOX activity.

In the above assays, we measured exogenous levels of O_2 that diffused from plant tissues to the media in the measurement cuvette. To determine whether we could also observe changed levels of O_2 inside plant tissues, we examined the O_2 status inside the central veins of leaf blades in situ using O_2 microsensors (Supplementary Figure S7a). Even though no statistical difference was detected in O_2 consumption rates between Col-0 and *rcd1*, O_2 re-accumulation after the start of illumination was suppressed in *rcd1* (Supplementary Figure S7b). This was in line with the measurements of external O_2 dynamics in seedlings.

Overall, the results indicated altered tissue O_2 levels and changes in the O_2-dependent chloroplastic processes in plant lines with deficient mitochondrial respiration, supporting the role of intracellular O_2 exchange in the studied organelle interaction.

Diverse mitochondrial defects increase abundance and respiration capacity of AOXs

A prominent feature of mitochondrial stress and the associated MDS transcriptional reprogramming is the induction of AOXs, enzymes that have been implicated in the regulation of cellular O_2 status. To evaluate the possible role of these enzymes in interregulation between mitochondria and chloroplasts, we quantified AOX protein abundance across the plant lines by immunoblotting with an antibody that recognizes all 5 Arabidopsis AOX isoforms (αAOX1/2, Supplementary Figure S8a). The antibody showed linear response in the range of 1.75 to 70 µg of total protein, making it

suitable for the quantitative comparison of plant lines with diverse AOX abundance (Supplementary Figure S8b). For most lines, differences in AOX abundance remained consistent between the seedling and mature growth stages (Supplementary Figure S8c). Several of the tested plant lines with mitochondrial defects demonstrated a statistically significant increase in AOX abundance compared to the wild type (Fig. 5a). For example, in *rcd1* AOX abundance was 8.7 ± 3.5 times higher, and in *ndufs4*, it was 7.8 ± 2.5 times higher than in Col-0 (Fig. 5a; Supplementary Dataset S1). We additionally assessed AOX respiration capacity by measuring changes in O_2 concentration in darkness in the presence of KCN, the inhibitor of COX respiration. AOX activity is resistant to KCN; hence, residual O_2 uptake in KCN-treated seedlings can be ascribed to AOXs. In several lines, application of KCN led to only minor drops in O_2 consumption, indicating strong involvement of AOX respiration in the overall O_2 uptake by the seedlings (Fig. 5b; Supplementary Figure S8d). For example, in Col-0, *rcd1* and *ndufs4*, KCN inhibited the O_2 consumption rate by 83 ± 15%, 17 ± 9%, and 42 ± 28%, respectively (Supplementary Figure S8d; Supplementary Dataset S1). For all tested lines, we found a correlation between AOX abundance and AOX capacity (Pearson correlation from averages 0.8704, $P < 0.0001$) (Fig. 5c). These results indicated that modified AOX respiration is a general response to diverse mitochondrial defects.

Roles of individual alternative respiratory enzymes in the organelle interaction

Taken together, the results suggested a link between AOX abundance, AOX respiration capacity, and various MV-related phenotypes. This connection could also be seen in a correlation analysis, where AOX abundance correlated with AOX respiration capacity, while all the described MV-related phenotypes correlated with each other (Fig. 6a), with the *AOX1a*-OE line being one notable exception (Supplementary Figure S9a). When this plant line was removed from the correlation analyses, a positive correlation was observed between AOX abundance, AOX capacity, and diverse MV phenotypes (Fig. 6a). Furthermore, resistance to MV-induced photoinhibition showed a positive correlation with O_2 consumption rate in darkness (Fig. 6a and b), and MV-related phenotypes also negatively correlated with O_2 re-accumulation rate in light, although with low statistical significance. Interestingly, in MV assays, the *AOX1a*-OE line performed similarly to the wild type, suggesting that enhanced expression of a single AOX1a isoform was not sufficient for the studied organellar interaction.

In *A. thaliana*, the repertoire of alternative respiratory enzymes includes 5 AOX isoforms (AOX1a, –1b, –1c, –1d, and –2) and 7 NDs (NDA1, –2; NDB1, –2, –3, –4; NDC1) (Møller et al. 2021). AOX1a and AOX1d are the main stress-inducible AOX isoforms in Arabidopsis leaves (Oh et al. 2022). To further assess their roles in the impact of respiration on chloroplasts, we generated an *aox1a aox1d* double mutant, which showed similar AOX capacity and MV-induced photoinhibition to Col-0 (Supplementary Figures S8d and S9b, respectively). Notably, immunoblotting with αAOX1/2 antibody still displayed another AOX isoform in *aox1a aox1d* (Supplementary Figure S9c). Thus, the studied effects of mitochondrial respiration on chloroplasts could not be linked to specific AOX isoform(s).

This result prompted us to examine whether other alternative respiratory enzymes contribute to the inter-organelle interaction. We quantified their gene expression using publicly available RNA transcriptome datasets for *gsnor1*, *lon1*, *mtran1 mtran2*, *phb3*, *rcd1* (2 independent datasets), and *rpoTmp*. Importantly, all the datasets showed increased expression of marker genes for induced MDS signaling: *UPOX* (AT2G21640) and *HRG2* (AT5G24640). Furthermore, in all datasets except *gsnor1*, we observed increased expression of hypoxia marker genes *ERF71* (AT2G47520), *HRU1* (AT3G03270), and *PDC1* (AT4G33070), with the strongest increase in *ERF71*. Almost all genes encoding AOXs and NDs (*NDC1* being the exception) showed significantly increased expression in at least one of the genetic perturbations (Fig. 6c). These transcriptomic results indicate that mitochondrial dysfunction triggers changes in the expression of not just *AOX*s, but a repertoire of alternative respiratory enzymes.

Taken together, these results suggest a link between stress-induced changes in mitochondrial respiration, tissue O_2 status, and the MV-catalyzed Mehler reaction. The contribution

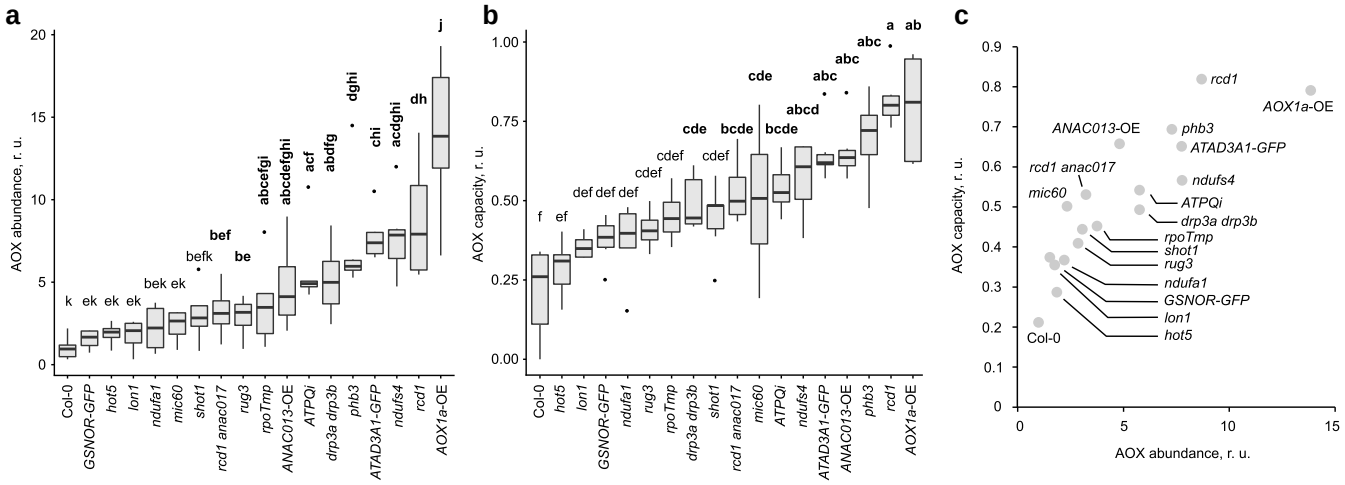

Figure 5. AOX abundance and capacity in plant lines with perturbed mitochondrial functions. AOX abundance was measured by immunoblotting total protein extracts from seedlings a), and AOX capacity was determined as the fraction of O_2 consumption that was not inhibited by KCN b). The box plots indicate the median (horizontal line), first and third quartiles (box), minimum and maximum (whiskers), and the genotypes are arranged in order of increasing mean. Statistically significant groups are indicated with letters, bolded for lines that are different from the wild type (Kruskal–Wallis test, $P < 0.05$). Quantification in a) was from 4 independent immunoblots and in b) from 6 independent biological replicates. Correlation between AOX abundance and capacity is displayed in c).

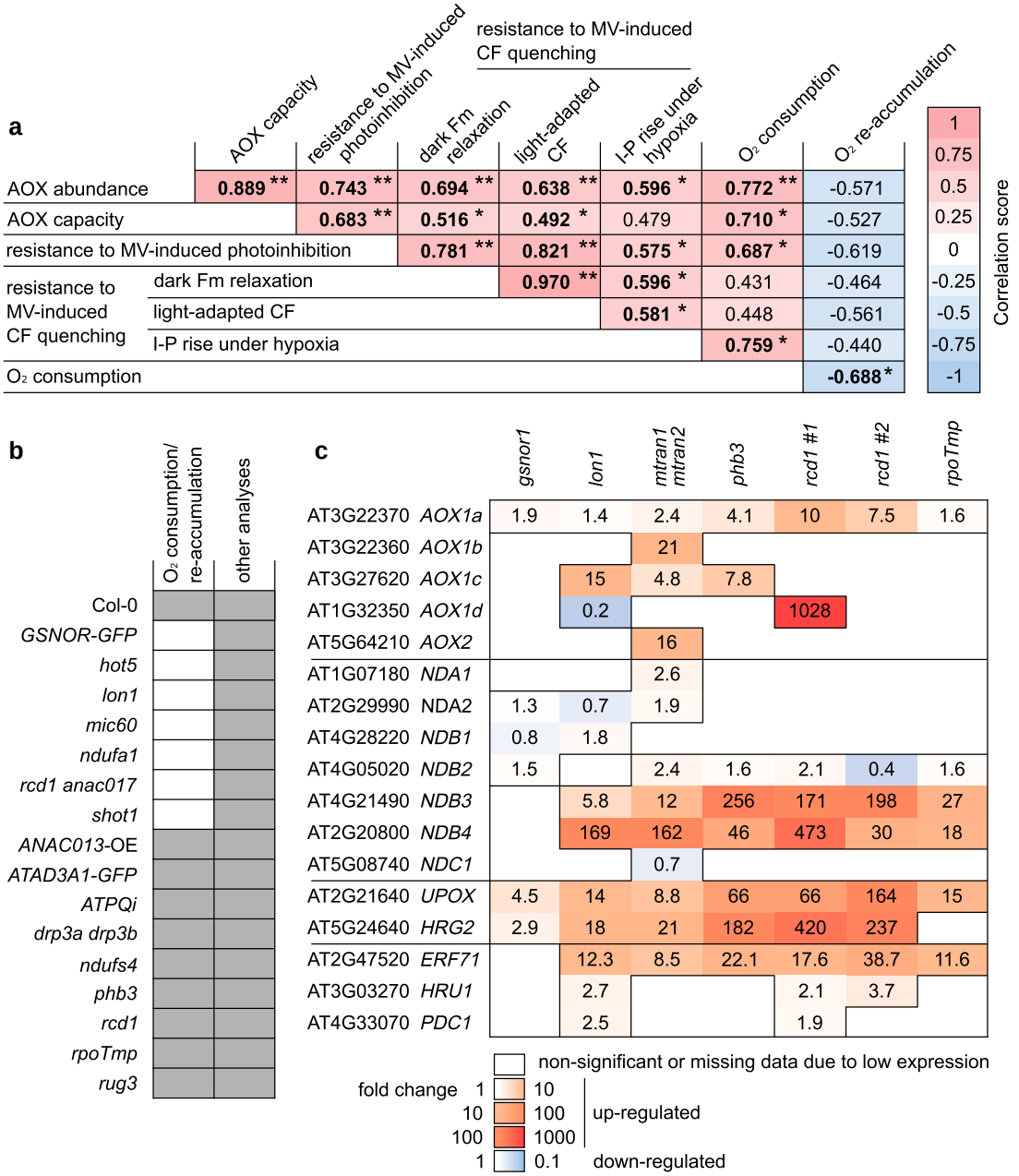

Figure 6. Correlation of chloroplastic and mitochondrial phenotypes and expression of alternative respiratory enzymes in plant lines with perturbed mitochondrial functions. Parameters associated with chloroplastic and mitochondrial phenotypes were analyzed using Pearson correlation, excluding the atypically behaving *AOX1a*-OE line a). Correlation values are bolded and marked with 1 or 2 asterisks to indicate significance at $P < 0.05$ and <0.01, respectively, and the color of the pane is used to indicate the strength and direction of correlation. Plant lines included in the correlation analyses in a) are listed in b). Details are available in Supplementary Dataset S1. c) Publicly available transcriptome datasets were re-analyzed to identify genes with significantly altered expression. Data are presented as the fold change in the mutant relative to the wild type. Displayed are *AOX*, *ND*, and marker genes for MDS (*UPOX* and *HRG2*), and hypoxia (*ERF71*, *HRU1*, *PDC1*). MV, methyl viologen; CF, chlorophyll fluorescence.

of individual mitochondrial respiratory components in this inter-organelle interaction remains to be refined.

Discussion

The emerging interaction of plant mitochondria and chloroplasts through intracellular O_2 exchange

We explored a link between mitochondrial respiration, altered tissue O_2 levels, and chloroplastic functions, particularly as related to ROS metabolism. Evidence for such interaction has accumulated across multiple studies. For example, hypoxic signaling influences transcriptional control of chlorophyll biosynthesis (Abbas et al. 2022), mitochondrial alternative respiratory components support photosynthetic activity (Jethva et al. 2022; Renziehausen et al. 2024), and chloroplastic ROS homeostasis is modified by the MDS pathway (De Clercq et al. 2013; Ng et al. 2013; Shapiguzov et al. 2019, 2020). These observations indicate that chloroplasts actively partner with mitochondria in responses to changing O_2 levels, yet the mechanistic connections remain

poorly understood. Analyses of plant lines with activated mitochondrial MDS signaling have not revealed structural changes in chloroplasts that could explain modified chloroplastic functions (Jaspers et al. 2009; Brosché et al. 2014; Shapiguzov et al. 2019). This suggests that mitochondria influence chloroplasts through operational changes, such as altered metabolic fluxes, redox shuttles, or gas exchange (Shapiguzov et al. 2019, 2020; Sipari et al. 2020).

Most studies have linked the effects of altered mitochondrial respiration on photosynthesis to electron sink activities of AOXs. By consuming reducing equivalents from mitochondria and, via redox shuttles, from chloroplasts, AOXs can limit ROS production in both organelles (Yoshida and Noguchi 2011; Vanlerberghe 2013; Bailleul et al. 2015; Dahal and Vanlerberghe 2017; Murik et al. 2019; Vanlerberghe et al. 2020; Møller et al. 2021; Oh et al. 2022). An inter-organellar electron transfer pathway, possibly involving a malate shuttle, was proposed to compete with the Mehler reaction at the PSI acceptor side in the *rcd1* mutant, which exhibits constitutive MDS activation and increased AOX abundance (Shapiguzov et al. 2019).

A complementary explanation for how mitochondria influence ROS metabolism, including ROS in the chloroplast, involves the oxygen-consuming activities of these organelles. This role of mitochondria has been linked to diurnal changes in O_2 availability in young Arabidopsis leaves (Triozzi et al. 2024), as well as to hypoxic niches in specialized tissues (Gupta et al. 2009, 2018; Rasmusson et al. 2009; Kelliher and Walbot 2012; Van Dongen and Licausi 2015 ; Weits et al. 2021; Iida et al. 2025). Studies in photosynthetic tissues are limited by technical challenges, as O_2 evolution during photosynthesis masks mitochondrial O_2 consumption in the light. To overcome this, we used 2 conditions that allowed us to observe this interaction: hypoxia and treatment with MV, a catalyst of the Mehler reaction. MV suppresses photosynthetic O_2 evolution, likely by perturbing redox regulation of the chloroplastic ATP synthase (Nikkanen et al. 2024), which enhances thylakoid lumen acidification, increases non-photochemical quenching, and thus inhibits PSII activity. Importantly, MV does not inhibit CO_2 evolution, suggesting that mitochondrial respiration remains active (Shapiguzov et al. 2020). These features create similarities between MV stress and hypoxia and make MV a useful tool for this study. By catalyzing the Mehler reaction, MV alters the PSI redox state and quenches chlorophyll fluorescence, providing measurable in vivo signals that were instrumental for this study (Figs. 2 and 3).

Our results support the hypothesis that increased mitochondrial respiration, potentially associated with enhanced AOX activity, modulates chloroplast functions by lowering intracellular O_2. The effect of altered mitochondrial respiration on O_2-dependent and MV-catalyzed PSI oxidation was observed as early as 20 min after exposure to exogenous hypoxia (Fig. 2c to f), suggesting that in addition to possible de novo transcriptional reprogramming induced by hypoxic treatment, preexisting metabolic changes caused by altered mitochondrial functions play a central role. A plausible explanation for these observations is that O_2 limitation caused by enhanced respiration suppressed the Mehler reaction at PSI, thereby affecting photosynthetic electron transfer and ROS/redox metabolism in the chloroplast.

O_2 sink roles of mitochondrial respiratory pathways

The interaction between mitochondrial and chloroplastic ROS metabolism was previously linked to the alternative respiratory pathway. This is supported by correlations between chloroplastic phenotypes and AOX abundance and capacity (Fig. 6) and by the observation that the AOX inhibitor SHAM alters photosynthetic electron flow and MV toxicity (Shapiguzov et al. 2019; Pascual et al. 2021). However, the interaction could not be ascribed to a specific AOX isoform. For example, the *AOX1a*-OE line does not display increased MV tolerance (Fig. 2; Shapiguzov et al. 2020), despite its high KCN-resistant AOX respiration (Fig. 5; Shapiguzov et al. 2019). Single mutants *aox1a*, *aox1c*, and *aox1d*, as well as the double mutant *aox1a aox1d*, all show wild-type-like responses to MV (Supplementary Figure S9b; Shapiguzov et al. 2020). Furthermore, no differences in response to MV were observed between *rcd1* and *rcd1 aox1a* (Shapiguzov et al. 2019, 2020). These results suggest functional redundancy among AOX isoforms and point to a complex contribution of various mitochondrial respiratory components to MV tolerance.

Indeed, the lines with induced MDS signaling exhibit a broad MDS transcriptional response, with induced expression of several AOX and ND isoforms, the latter likely complementing AOX activities (Sweetman et al. 2019) (Fig. 6c). NO metabolism adds further complexity: AOXs reduce electron leakage to nitrite under normoxia, suppressing NO formation, while under hypoxia, over-reduced mitochondria can generate NO, which inhibits COX. Increased NO emission under hypoxia was reported in AOX-overexpressing lines (Vishwakarma et al. 2018; Jayawardhane et al. 2020), suggesting interplay between AOX and COX via NO. However, in our assays, the *hot5* mutant and *GSNOR-GFP* line showed largely wild-type-like responses, indicating that NO is not central to this interaction. The complexity of the above regulatory network likely explains the controversial performance of the *AOX1a*-OE transgenic line. While overexpression of AOX1a alone is sufficient to confer KCN-resistant respiration, it is insufficient to reproduce the physiological changes observed in other lines with mitochondrial defects.

Metabolic profiling of *rcd1* revealed increased respiratory flux (Shapiguzov et al. 2019) and altered pools of primary metabolites, many of which are mitochondrial substrates (Sipari et al. 2020). Hence, the molecular basis of mitochondrial O_2 sink capacity, and its impact on chloroplasts, is likely context-dependent and shaped by the flexibility of different respiratory branches (Sweetlove et al. 2010; Møller et al. 2021).

Possible implications and open questions

We performed direct measurements of tissue O_2 status and chloroplastic phenotypes in a set of Arabidopsis mutants and transgenic lines with diverse mitochondrial defects. Our study proposes a mechanistic link between mitochondrial O_2 consumption and chloroplast metabolism. While this interaction was revealed under artificial conditions using hypoxic atmosphere and MV treatment, the constitutively altered redox states of chloroplast thiol enzymes in *rcd1* suggest that the link is also relevant under natural conditions (Shapiguzov et al. 2019, 2020). A recent study showed daily O_2 fluctuations in young Arabidopsis leaves, with depletion at night due to respiration and accumulation during the day driven by photosynthesis (Triozzi et al. 2024). The effects of stressed mitochondrial respiration on these dynamics remain to be explored.

The results of this study highlight the Mehler reaction as a key link coordinating respiration and photosynthesis. The Mehler reaction controls chloroplast thiol redox states, thereby regulating processes such as carbon fixation, sugar metabolism, and ATP production. It may be required for activating photosynthetic electron transfer during the dark-to-light transition (Hani et al. 2024),

and it influences numerous signaling pathways dependent on chloroplast-derived ROS (Shapiguzov et al. 2012; Wang et al. 2020). For instance, chloroplastic ROS are sensed by the nuclear co-regulator RCD1, which interacts with transcription factors including ANAC013/ANAC016/ANAC017 (mitochondrial signaling), ERFVIIs (low-O_2 signaling), and PIFs (light signaling) (Jaspers et al. 2009; Shapiguzov et al. 2019; Vainonen et al. 2023). Furthermore, through its effect on photoassimilation, the Mehler reaction impacts sugar signaling via SnRK1 and TOR pathways, which merge with hypoxic signaling (Kunkowska et al. 2023). Future studies should explore how mitochondrial O_2 consumption shapes ROS signaling across organelles and compartments, including the apoplast and nucleus (Shapiguzov et al. 2012; Waszczak et al. 2018).

Our findings open opportunities for phenotyping plant respiration. In situ measurement of mitochondrial respiration is challenging due to the lack of direct spectroscopic markers. However, we show that mitochondrial activity can influence chlorophyll fluorescence under certain conditions, providing an opportunity to infer respiratory traits via spectroscopic approaches. This could form the basis for imaging tools to monitor plant respiration.

Materials and methods

Plant material and growth conditions

Arabidopsis (*A. thaliana*) was used in all experiments. Plants were grown on either 1:1 mix of soil and vermiculite in 12 h photoperiod with 200 to 250 µmol m^{-2} s^{-1} illumination (low light growth conditions) or on MS plates (full-strength MS medium, 0.6% gel, 3 mM MES hydrate) in 12 h photoperiod with 200 µmol m^{-2} s^{-1} illumination. The following mutants were used in the experiments: knockout mutants *rcd1-4* (AT1G32230), *rcd1-1 anac017* (AT1G32230/AT1G34190; Ng et al. 2013; Shapiguzov et al. 2019), *shot1-2* (AT3G60400; Kim et al. 2012), *hot5-2* (AT5G43940; Feechan et al. 2005; Lee et al. 2008), *rpoTmp-1* (AT5G15700; Kühn et al. 2009), *lon1-2* (AT5G26860; Rigas et al. 2009), *drp3a drp3b* (AT4G33650/AT2G14120; Fujimoto et al. 2009), *ndufa1* (AT3G08610; Meyer et al. 2011), *ndufs4* (AT5G67590; Meyer et al. 2009), *rug3-1* (AT5G60870; Kühn et al. 2011), *phb3* (AT5G40770; Van Aken et al. 2007), *mic60-1* (AT4G39690; Michaud et al. 2016), *cat2* (AT4G35090; Queval et al. 2007), *gox1*, *cat2 gox1* (AT4G35090/AT3G14420; Kerchev et al. 2016), and *rcd1 cat2* (Kaurilind et al. 2015). The double mutant *aox1a aox1d* was generated by crossing the single mutant lines *aox1a* (AT3G22370; Umbach et al. 2005) and *aox1d* (AT1G32350; GK-529D11). Transgenic lines included *atad3a1 atad3b1*: *ATAD3A1-GFP* (AT3G03060; Kim et al. 2021), *GSNOR-GFP* (AT5G43940; Xu et al. 2013), *AOX1a* overexpressor (AT3G22370; Umbach et al. 2005), *ANAC013* overexpressor (AT1G32870; De Clercq et al. 2013), and RNAi mutant *ATPQi* (AT3G52300; Liu et al. 2021). All mutants and transgenic lines are in Columbia-0 (Col-0) background.

Chlorophyll fluorescence imaging

Chlorophyll fluorescence imaging assays were performed with leaf discs that were prepared similarly for all measurements. Leaf discs were placed on the surface of ultrapure water with 0.05% Tween-20, in the presence or absence of MV in the concentrations indicated in figure panels. The discs were then incubated in darkness to facilitate uptake of MV for approximately 16 h before imaging. To minimize the effects of MV on photosynthesis, precautions were taken not to expose plant material to any light prior to measurements.

MV-induced photoinhibition and quenching of Fm and light-adapted chlorophyll fluorescence were assessed by chlorophyll fluorescence imaging using IMAGING-PAM M-Series (Heinz Walz, Effeltrich, Germany). Photoinhibition protocols are described in Shapiguzov and Kangasjärvi (2022). In brief, MV toxicity in leaf discs, prepared as described above, was induced by repetitive 1-h light periods (450 nm, 80 µmol m^{-2} s^{-1}) each followed by a 20 min dark period, then Fo and Fm measurements. The resulting decay of maximal quantum yield of PSII was calculated as Fv/Fm = (Fm – Fo)/Fm. Chlorophyll fluorescence quenching routines are described in Shapiguzov et al. (2020). In brief, a hypoxic environment was introduced by flushing nitrogen gas over the prepared leaf discs: first for 20 min in darkness to acclimate the leaf discs, then continuously through the experiment. Imaging of chlorophyll fluorescence was conducted under a saturating light pulse (Fm relaxation measurement) followed by low-intensity actinic light (450 nm, 80 µmol m^{-2} s^{-1}; light-adapted fluorescence measurement). For flash-induced chlorophyll fluorescence imaging, we used PlantScreen SC Mobile System equipped with ultra-fast CMOS camera TOMI 3 with 20 µs maximal frame rate of image acquisition (Photon Systems Instruments, Drásov, Czechia). Imaging protocols are described in Shapiguzov et al. (2020). In brief, samples were placed in an airtight container that was continuously flooded with nitrogen gas, and the measurements were performed through the transparent cover for hypoxic measurements. The time of exposure to nitrogen gas was adjusted to reach a steady state chlorophyll fluorescence response. For each assay, we used leaf discs from at least 4 to 5 independent plants (for MV-treated samples) or 3 independent plants (for control samples), and the experiments were repeated twice (photoinhibition and light-adapted fluorescence measurements) or 3 times (Fm relaxation and flash-induced chlorophyll fluorescence imaging measurements), with similar results.

P700 oxidation measurements

P700 analyses were done as described in Shapiguzov et al. (2019). The detached leaves were placed on the surface of ultrapure water with 0.05% Tween-20, in the presence or absence of 1 µM MV and incubated overnight in darkness. For the generation of a hypoxic atmosphere, the leaves were next placed into transparent plastic bags with or without an AnaeroGen hypoxia generator. Soda lime granules were added to the bags, as described in Shapiguzov et al. (2020), to avoid the possible effects of CO_2 generated by the reaction. The leaves were kept inside the bags for 4 h in darkness, after which light treatments and spectroscopic measurements were performed through the plastic using DUAL-PAM-100 (Walz, Germany).

Shoot tissue O_2 consumption and production

Shoot tissue O_2 dynamics were measured using the MicroRespiration system (Unisense, Denmark). Plants were grown on MS plates for approximately 3 weeks. Their aerial parts were cut off, weighed to obtain fresh mass, and inserted into 2 mL glass vials, which were filled with analysis buffer (Smart and Barko solution, 0.6 mM $MgSO_4$, 0.8 mM $CaCl_2$, 1 mM $KHCO_3$ supplemented with 5 mM MES monohydrate). To restrict photorespiration as O_2 builds up inside the vial, the analysis buffer was partially deoxygenated by mixing at 1:1 ratio O_2-saturated buffer and buffer that had been deoxygenated by bubbling it with nitrogen gas, resulting in an initial O_2 concentration of approximately 150 to 200 µmol/L.

The vials were placed in a rack inside a constant temperature bath (37 °C), and O_2 concentrations were monitored through a capillary in the glass lid with an optode (OPTO-MR, Unisense Denmark) using LOGGER (Unisense, Denmark) at a rate of 1 Hz while the plants were treated to the following regime: vials were kept in darkness until O_2 concentrations in all vials had been reduced to <10 µmol/L, or until the O_2 concentration in at least one vial had remained at <1 µmol/L for at most 20 min. After this, the vials were illuminated (30 µmol m^{-2} s^{-1}) until the O_2 concentrations within vials had plateaued, or at most 2 h. O_2 concentrations were recorded with RATE (Unisense, Denmark), and O_2 consumption in darkness as well as re-accumulation in light were normalized to fresh sample mass. At least 5 biological replicates were measured, with the exception of *drp3a drp3b* and *rug3* (3 replicates each). For measurements in the presence of SHAM, either dimethyl sulfoxide (DMSO; control) or 8 mM SHAM was added to the analysis buffer at the beginning of the measurement. Contamination between samples was avoided by rinsing the O_2 optode in fresh buffer after SHAM-containing samples were measured.

Leaf tissue O_2 dynamics

O_2 status of intact leaves submerged in deoxygenated medium was measured using Clark-type O_2 microsensors (Unisense, Denmark). Whole leaves were excised, kept submerged in 0.05% Tween-20 solution overnight (12 to 16 h) in darkness, and placed over a firm foam with the main vein facing upwards. A solid piece of plastic with a hole in the center was positioned over the leaf, the sandwiched leaf was attached firmly to a metal mesh with rubber bands and placed inside a container (200 × 100 × 100 mm, in total 2 L). An O_2 microsensor (OX-10, Unisense, Denmark) was inserted 80 to 100 µm into the main vein of the leaf lamina, with 0 indicating the tissue surface. Stagnant, deoxygenated buffer solution (0.1% agar) was added to the container and O_2 concentration on the adaxial side of leaf central vein was recorded using LOGGER (Unisense, Denmark) at a rate of 1 Hz. The initial part of the measurement was conducted in darkness, until the O_2 concentration declined and remained at a steady state below 5 µmol/L. Then, a light was turned on (ca. 15 µmol m^{-2} s^{-1}) and O_2 concentration was measured until it reached a plateau. The O_2 concentration and temperature of the external medium were monitored using an O_2 minioptode (OPTO-MR, Unisense, Denmark) and a temperature probe (ZNTC, Unisense, Denmark). The positioning of the microsensor was aided by a motorized micromanipulator controlled by LOGGER and visually aided with a dissection microscope (WILD M3B, Leica, Switzerland).

Protein abundance measurements

Total AOX abundance was determined by immunoblotting. Untreated plants were grown on either MS plates for 18 d and collected whole, or on soil for 21 d and their leaves were collected. Plant tissue was ground in liquid nitrogen, and proteins were extracted by incubating the samples for 20 min at 37 °C in lysis buffer (2% SDS, 20 mM Tris-HCl pH 7.8 supplemented with protease inhibitor cocktail P9599, Sigma-Aldrich). After centrifugation for 5 min at 15,000 g, the samples were suspended in Laemmli buffer. Protein amounts were normalized to total protein (52.3 µg/well) or fresh plant mass (5 mg/well) for whole leaves and seedlings, respectively. The extracts were separated on a 12% SDS-PAGE gel and transferred to Bio-Rad Immun-blot PVDF membrane. AOX was detected with an αAOX1/2 antibody (AS04 054, dil. 1:5,000, Agrisera), PSI with an αPsaA antibody (AS06 172, dil. 1:5,000, Agrisera), together with an HRP-tagged secondary antibody (ECL anti-rabbit IgG LNA934V/AH, GE Healthcare), and detected using a UVP Biospectrum 610 imaging system. For total protein estimations, the membranes were stained with amido black. Band intensities were calculated with the gel analyzer in ImageJ. Quantification was done using 4 independent immunoblots.

Measurements of O_2 consumption rates in the presence of respiration inhibitors

For measurements of plant O_2 consumption in the presence of respiration inhibitors, plants were grown for 18 d on MS plates, and aerial parts were cut off, weighed (approximately 20 mg/sample), and placed in an Oxygraph measurement chamber (Hansatech instruments) in air-saturated liquid MS medium. Oxygen consumption in darkness was monitored with a Clark-type O_2 electrode until it stabilized, for approximately 15 min. After this, changes in O_2 consumption were measured in the presence of respiration inhibitors by injecting potassium cyanide (KCN, 4 mM) into the measurement chamber, waiting for the signal to stabilize, then adding SHAM (2 mM) in the same manner. Respiratory parameters were processed with the Oxygraph plus software, and relative O_2 consumption rates were determined by normalizing the rates to plant mass. Six biological replicates were measured for each plant line.

Transcriptome analyses

RNA sequence data were acquired from the publicly available NCBI GEO Datasets (https://www.ncbi.nlm.nih.gov/geo/) for the following Arabidopsis mutant lines with compromised mitochondria: *mtran1 mtran2* (Tran et al. 2023), *phb3* and *rpoTmp* (Van Aken et al. 2016), 2 datasets with *rcd1* (Wirthmueller et al. 2018; Tao et al. 2023), *gsnor1* (Pan and Cui 2021), and *lon1* (Song et al. 2024). Only datasets with at least 3 biological replicates were included in the analysis. For the paired-end sequences, each read end was processed individually while retaining pairing information. The raw sequencing data underwent quality control using FastQC (Andrews 2010), followed by sequence trimming using Trimmomatic (Bolger et al. 2014), to remove low-quality bases when necessary. Potential contamination from ribosomal RNA was removed with sortmeRNA (Kopylova et al. 2012). The trimmed reads were then aligned using STAR with the latest available Arabidopsis transcriptome reference (AtRTD3) (Zhang et al. 2022). Differentially expressed genes were identified using the DESeq2 package in RStudio (Love et al. 2014).

Statistical analyses

Statistical analyses of all results were conducted with SPSS (IBM, USA). Differences between variances were estimated with ANOVA or Kruskal–Wallis, depending on the normality and equality distributions of the samples. Correlation from average values was measured with Bonferroni-corrected Pearson. Standard cutoff limit for statistically significant *P*-value (0.05) was used for all experiments except correlation, where *P*-value 0.01 was used as well. The box and whisker plots included in figures show the median (horizontal line), the first and third quartiles (box), minimum and maximum (whiskers), and outliers, defined as third quartile + 1.5 × interquartile range and first quartile − 1.5 × interquartile range (dots). Raw data and statistics are presented in Supplementary Dataset S1.

Accession numbers

TAIR gene identifiers corresponding to the mutants and overexpressor lines used in the study are listed in Materials and methods, *Plant material and growth conditions*. NCBI GEO datasets used for transcriptome analyses are listed in Materials and methods, *Transcriptome analyses*.

Acknowledgments

The authors dedicate this study to the memory of Prof. Jaakko Kangasjärvi. We thank Prof. Romy Schmidt-Schippers for the advice on the studies of hypoxia and for her critical comments on the manuscript. We thank Dr. Cezary Waszczak for sharing the seeds of photorespiratory mutants and Dr. Julia Vainonen for the help in the preparation of this manuscript.

Author contributions

M.P., B.B., O.B., L.L.P.O., M.K., M.B., L.N., E.V., O.P., and A.S. conceived and designed experiments. M.P., B.B., L.L.P.O., M.K., M.B., L.N., and A.S. carried out experiments. All authors analyzed the results. A.S. and M.P. wrote the article. All authors read and contributed to the final article.

Supplementary material

The following materials are available in the online version of this article.

Supplementary Dataset S1. Source Data and Statistical Analyses

Supplementary Figure S1. Light-dependence of methyl viologen (MV) toxicity in the studied lines.

Supplementary Figure S2. Quenching of chlorophyll fluorescence under control conditions.

Supplementary Figure S3. MV-induced photoinhibition under different photorespiratory conditions.

Supplementary Figure S4. MV-induced photoinhibition in mutant lines with altered photorespiration.

Supplementary Figure S5. Flash-induced chlorophyll fluorescence measurements in control conditions.

Supplementary Figure S6. O_2 consumption dynamics in plant lines with perturbed mitochondrial functions in the presence of AOX inhibitor SHAM.

Supplementary Figure S7. O_2 dynamics inside leaf tissue.

Supplementary Figure S8. AOX abundance and capacity measurements.

Supplementary Figure S9. Characterization of the lines with genetically altered AOX levels.

Funding

This work was supported by the Research Council of Finland (decision 346140, Centre of Excellence in Tree Biology; A.S.). Development of *ATAD3-GFP*, *ATPd* RNAi line, *hot5-2*, and *GSNOR-GPF* lines were supported by the National Science Foundation grants IOS 1354960 and MCB 1517046 to E.V.

Conflict of interest statement. The authors declare that there are no conflicts of interest.

Data availability

The data generated in this study are included in this article and the online supplementary material.

References

Abbas M et al. An oxygen-sensing mechanism for angiosperm adaptation to altitude. *Nature*. 2022:606:565–569. https://doi.org/10.1038/s41586-022-04740-y.

Andrews S. FastQC: a quality control tool for high throughput sequence data [online]. http://www.bioinformatics.babraham.ac.uk/projects/fastqc/

Bailey-Serres J, Geigenberger P, Perata P, Sasidharan R, Schwarzländer M. Hypoxia as challenge and opportunity: from cells to crops, to synthetic biology. *Plant Physiol*. 2024:197:kiae640. https://doi.org/10.1093/plphys/kiae640.

Bailleul B et al. Energetic coupling between plastids and mitochondria drives CO2 assimilation in diatoms. *Nature*. 2015:524:366–369. https://doi.org/10.1038/nature14599.

Bauwe H, Hagemann M, Fernie AR. Photorespiration: players, partners and origin. *Trends Plant Sci*. 2010:15:330–336. https://doi.org/10.1016/j.tplants.2010.03.006.

Bolger AM, Lohse M, Usadel B. Trimmomatic: a flexible trimmer for Illumina sequence data. *Bioinformatics*. 2014:30:2114–2120. https://doi.org/10.1093/bioinformatics/btu170.

Brosché M et al. Transcriptomics and functional genomics of ROS-induced cell death regulation by RADICAL-INDUCED CELL DEATH1. *PLoS Genet*. 2014:10:e1004112. https://doi.org/10.1371/journal.pgen.1004112.

Dahal K, Vanlerberghe GC. Alternative oxidase respiration maintains both mitochondrial and chloroplast function during drought. *New Phytol*. 2017:213:560–571. https://doi.org/10.1111/nph.14169.

De Clercq I et al. The membrane-bound NAC transcription factor ANAC013 functions in mitochondrial retrograde regulation of the oxidative stress response in Arabidopsis. *Plant Cell*. 2013:25:3472–3490. https://doi.org/10.1105/tpc.113.117168.

Eysholdt-Derzsó E et al. Endoplasmic reticulum-bound ANAC013 factor is cleaved by RHOMBOID-LIKE 2 during the initial response to hypoxia in Arabidopsis thaliana. *Proc Natl Acad Sci U S A*. 2023:120:e2221308120. https://doi.org/10.1073/pnas.2221308120.

Farrington JA, Ebert M, Land EJ, Fletcher K. Bipyridylium quaternary salts and related compounds. V. Pulse radiolysis studies of the reaction of paraquat radical with oxygen. Implications for the mode of action of bipyridyl herbicides. *Biochim Biophys Acta*. 1973:314:372–381. https://doi.org/10.1016/0005-2728(73)90121-7.

Feechan A et al. A central role for S-nitrosothiols in plant disease resistance. *Proc Natl Acad Sci U S A*. 2005:102:8054–8059. https://doi.org/10.1073/pnas.0501456102.

Fujimoto M et al. Arabidopsis dynamin-related proteins DRP3A and DRP3B are functionally redundant in mitochondrial fission, but have distinct roles in peroxisomal fission. *Plant J*. 2009:58:388–400. https://doi.org/10.1111/j.1365-313X.2009.03786.x.

Gupta KJ, Kumari A, Florez-Sarasa I, Fernie AR, Igamberdiev AU. Interaction of nitric oxide with the components of the plant mitochondrial electron transport chain. *J Exp Bot*. 2018:69:3413–3424. https://doi.org/10.1093/jxb/ery119.

Gupta KJ, Zabalza A, van Dongen JT. Regulation of respiration when the oxygen availability changes. *Physiol Plant*. 2009:137:383–391. https://doi.org/10.1111/j.1399-3054.2009.01253.x.

Hani U et al. A complex and dynamic redox network regulates oxygen reduction at photosystem I in Arabidopsis. *Plant Physiol*. 2024:197:kiae501. https://doi.org/10.1093/plphys/kiae501.

Iida H et al. Plants monitor the integrity of their barrier by sensing gas diffusion. *Nature*. 2025:644:483–489. https://doi.org/10.1038/s41586-025-09223-4.

Jaspers P et al. Unequally redundant RCD1 and SRO1 mediate stress and developmental responses and interact with transcription factors. *Plant J*. 2009:60:268–279. https://doi.org/10.1111/j.1365-313X.2009.03951.x.

Jayawardhane J et al. Roles for plant mitochondrial alternative oxidase under normoxia, hypoxia, and reoxygenation conditions. *Front Plant Sci*. 2020:11:566. https://doi.org/10.3389/fpls.2020.00566.

Jethva J, Schmidt RR, Sauter M, Selinski J. Try or die: dynamics of plant respiration and how to survive low oxygen

conditions. *Plants (Basel)*. 2022:11:205. https://doi.org/10.3390/plants11020205.

Kaurilind E, Xu E, Brosché M. A genetic framework for H_2O_2 induced cell death in *Arabidopsis thaliana*. *BMC Genomics*. 2015:16:837. https://doi.org/10.1186/s12864-015-1964-8.

Kelliher T, Walbot V. Hypoxia triggers meiotic fate acquisition in maize. *Science*. 2012:337:345–348. https://doi.org/10.1126/science.1220080.

Kerchev P et al. Lack of GLYCOLATE OXIDASE1, but not GLYCOLATE OXIDASE2, attenuates the photorespiratory phenotype of CATALASE2-deficient Arabidopsis. *Plant Physiol*. 2016:171:1704–1719. https://doi.org/10.1104/pp.16.00359.

Khan K et al. Mitochondria-derived reactive oxygen species are the likely primary trigger of mitochondrial retrograde signaling in Arabidopsis. *Curr Biol*. 2024:34:327–342.e4. https://doi.org/10.1016/j.cub.2023.12.005.

Kim M et al. mTERF18 and ATAD3 are required for mitochondrial nucleoid structure and their disruption confers heat tolerance in Arabidopsis thaliana. *New Phytol*. 2021:232:2026–2042. https://doi.org/10.1111/nph.17717.

Kim M, Lee U, Small I, des Francs-Small CC, Vierling E. Mutations in an Arabidopsis mitochondrial transcription termination factor-related protein enhance thermotolerance in the absence of the major molecular chaperone HSP101. *Plant Cell*. 2012:24:3349–3365. https://doi.org/10.1105/tpc.112.101006.

Kopylova E, Noé L, Touzet H. SortMeRNA: fast and accurate filtering of ribosomal RNAs in metatranscriptomic data. *Bioinformatics*. 2012:28:3211–3217. https://doi.org/10.1093/bioinformatics/bts611.

Kühn K et al. Phage-type RNA polymerase RPOTmp performs gene-specific transcription in mitochondria of Arabidopsis thaliana. *Plant Cell*. 2009:21:2762–2779. https://doi.org/10.1105/tpc.109.068536.

Kühn K et al. The RCC1 family protein RUG3 is required for splicing of nad2 and complex I biogenesis in mitochondria of Arabidopsis thaliana. *Plant J*. 2011:67:1067–1080. https://doi.org/10.1111/j.1365-313X.2011.04658.x.

Kunkowska AB et al. Target of rapamycin signaling couples energy to oxygen sensing to modulate hypoxic gene expression in Arabidopsis. *Proc Natl Acad Sci U S A*. 2023:120:e2212474120. https://doi.org/10.1073/pnas.2212474120.

Lee U, Wie C, Fernandez BO, Feelisch M, Vierling E. Modulation of nitrosative stress by S-nitrosoglutathione reductase is critical for thermotolerance and plant growth in Arabidopsis. *Plant Cell*. 2008:20:786–802. https://doi.org/10.1105/tpc.107.052647.

Liu T, Arsenault J, Vierling E, Kim M. Mitochondrial ATP synthase subunit d, a component of the peripheral stalk, is essential for growth and heat stress tolerance in Arabidopsis thaliana. *Plant J*. 2021:107:713–726. https://doi.org/10.1111/tpj.15317.

Love MI, Huber W, Anders S. Moderated estimation of fold change and dispersion for RNA-seq data with DESeq2. *Genome Biol*. 2014:15:550. https://doi.org/10.1186/s13059-014-0550-8.

Meyer EH et al. Remodeled respiration in ndufs4 with low phosphorylation efficiency suppresses Arabidopsis germination and growth and alters control of metabolism at night. *Plant Physiol*. 2009:151:603–619. https://doi.org/10.1104/pp.109.141770.

Meyer EH, Solheim C, Tanz SK, Bonnard G, Millar AH. Insights into the composition and assembly of the membrane arm of plant complex I through analysis of subcomplexes in Arabidopsis mutant lines. *J Biol Chem*. 2011:286:26081–26092. https://doi.org/10.1074/jbc.M110.209601.

Michaud M et al. Atmic60 is involved in plant mitochondria lipid trafficking and is part of a large complex. *Curr Biol*. 2016:26:627–639. https://doi.org/10.1016/j.cub.2016.01.011.

Miyake C. Alternative electron flows (water-water cycle and cyclic electron flow around PSI) in photosynthesis: molecular mechanisms and physiological functions. *Plant Cell Physiol*. 2010:51:1951–1963. https://doi.org/10.1093/pcp/pcq173.

Møller IM, Rasmusson AG, Van Aken O. Plant mitochondria—past, present and future. *Plant J*. 2021:108:912–959. https://doi.org/10.1111/tpj.15495.

Murik O et al. Downregulation of mitochondrial alternative oxidase affects chloroplast function, redox status and stress response in a marine diatom. *New Phytol*. 2019:221:1303–1316. https://doi.org/10.1111/nph.15479.

Nawrocki WJ, Tourasse NJ, Taly A, Rappaport F, Wollman F-A. The plastid terminal oxidase: its elusive function points to multiple contributions to plastid physiology. *Annu Rev Plant Biol*. 2015:66:49–74. https://doi.org/10.1146/annurev-arplant-043014-114744.

Ng S et al. A membrane-bound NAC transcription factor, ANAC017, mediates mitochondrial retrograde signaling in Arabidopsis. *Plant Cell*. 2013:25:3450–3471. https://doi.org/10.1105/tpc.113.113985.

Nikkanen L et al. PGR5 is needed for redox-dependent regulation of ATP synthase both in chloroplasts and in cyanobacteria. bioRxiv 621747. https://doi.org/10.1101/2024.11.03.621747, preprint; not peer reviewed.

Nishiyama Y, Allakhverdiev SI, Murata N. Protein synthesis is the primary target of reactive oxygen species in the photoinhibition of photosystem II. *Physiol Plant*. 2011:142:35–46. https://doi.org/10.1111/j.1399-3054.2011.01457.x.

Oh GGK, O'Leary BM, Signorelli S, Millar AH. Alternative oxidase (AOX) 1a and 1d limit proline-induced oxidative stress and aid salinity recovery in Arabidopsis. *Plant Physiol*. 2022:188:1521–1536. https://doi.org/10.1093/plphys/kiab578.

Ojeda V, Pérez-Ruiz JM, Cejudo FJ. 2-Cys peroxiredoxins participate in the oxidation of chloroplast enzymes in the dark. *Mol Plant*. 2018:11:1377–1388. https://doi.org/10.1016/j.molp.2018.09.005.

Pan Q, Cui B. RNA-sequence of *Arabidopsis thaliana* lines *gsnor1* and Col-0 post infection of *Phytophthora parasitica* against controls. BioStudies, E-MTAB-8845. https://www.ebi.ac.uk/biostudies/arrayexpress/studies/E-MTAB-8845

Pascual J et al. ACONITASE 3 is part of theANAC017 transcription factor-dependent mitochondrial dysfunction response. *Plant Physiol*. 2021:186:1859–1877. https://doi.org/10.1093/plphys/kiab225.

Queval G et al. Conditional oxidative stress responses in the Arabidopsis photorespiratory mutant *cat2* demonstrate that redox state is a key modulator of daylength-dependent gene expression, and define photoperiod as a crucial factor in the regulation of H_2O_2-induced cell death. *Plant J*. 2007:52:640–657. https://doi.org/10.1111/j.1365-313X.2007.03263.x.

Rasmusson AG, Fernie AR, van Dongen JT. Alternative oxidase: a defence against metabolic fluctuations? *Physiol Plant*. 2009:137:371–382. https://doi.org/10.1111/j.1399-3054.2009.01252.x.

Renziehausen T, Chaudhury R, Hartman S, Mustroph A, Schmidt-Schippers RR. A mechanistic integration of hypoxia signaling with energy, redox, and hormonal cues. *Plant Physiol*. 2024:197:kiae596. https://doi.org/10.1093/plphys/kiae596.

Rigas S et al. Role of Lon1 protease in post-germinative growth and maintenance of mitochondrial function in Arabidopsis thaliana. *New Phytol*. 2009:181:588–600. https://doi.org/10.1111/j.1469-8137.2008.02701.x.

Schreiber U. Light-induced changes of far-red excited chlorophyll fluorescence: further evidence for variable fluorescence of

photosystem I in vivo. *Photosynth Res*. 2023:155:247–270. https://doi.org/10.1007/s11120-022-00994-9.

Schreiber U, Klughammer C. Evidence for variable chlorophyll fluorescence of photosystem I in vivo. *Photosynth Res*. 2021:149:213–231. https://doi.org/10.1007/s11120-020-00814-y.

Shameer S, Ratcliffe RG, Sweetlove LJ. Leaf energy balance requires mitochondrial respiration and export of chloroplast NADPH in the light. *Plant Physiol*. 2019:180:1947–1961. https://doi.org/10.1104/pp.19.00624.

Shapiguzov A et al. Arabidopsis RCD1 coordinates chloroplast and mitochondrial functions through interaction with ANAC transcription factors. *eLife*. 2019:8:e43284. https://doi.org/10.7554/eLife.43284.

Shapiguzov A et al. Dissecting the interaction of photosynthetic electron transfer with mitochondrial signalling and hypoxic response in the Arabidopsis rcd1 mutant. *Philos Trans R Soc Lond B Biol Sci*. 2020:375:20190413. https://doi.org/10.1098/rstb.2019.0413.

Shapiguzov A, Kangasjärvi J. Studying plant stress reactions in vivo by PAM chlorophyll fluorescence imaging. *Methods Mol Biol*. 2022:2526:43–61. https://doi.org/10.1007/978-1-0716-2469-2_4.

Shapiguzov A, Vainonen JP, Wrzaczek M, Kangasjärvi J. ROS-talk—how the apoplast, the chloroplast, and the nucleus get the message through. *Front Plant Sci*. 2012:3:292. https://doi.org/10.3389/fpls.2012.00292.

Sipari N, Lihavainen J, Shapiguzov A, Kangasjärvi J, Keinänen M. Primary metabolite responses to oxidative stress in early-senescing and paraquat resistant Arabidopsis thaliana rcd1 (radical-induced cell death1). *Front Plant Sci*. 2020:11:194. https://doi.org/10.3389/fpls.2020.00194.

Song C et al. Protein aggregation in plant mitochondria lacking Lon1 inhibits translation and induces unfolded protein responses. *Plant Cell Environ*. 2024:47:4383–4397. https://doi.org/10.1111/pce.15035.

Stirbet A, Govindjee. On the relation between the Kautsky effect (chlorophyll a fluorescence induction) and photosystem II: basics and applications of the OJIP fluorescence transient. *J Photochem Photobiol B*. 2011:104:236–257. https://doi.org/10.1016/j.jphotobiol.2010.12.010.

Stirbet A, Govindjee. Chlorophyll a fluorescence induction: a personal perspective of the thermal phase, the J-I-P rise. *Photosynth Res*. 2012:113:15–61. https://doi.org/10.1007/s11120-012-9754-5.

Strasser RJ, Tsimilli-Michael M, Srivastava A. Analysis of the chlorophyll a fluorescence transient. In: Papageorgiou GC, Govindjee, editors. *Chlorophyll a fluorescence. Advances in photosynthesis and respiration*. 2004:vol 19. Springer. p. 321–362. https://doi.org/10.1007/978-1-4020-3218-9_12.

Sweetlove LJ, Beard KF, Nunes-Nesi A, Fernie AR, Ratcliffe RG. Not just a circle: flux modes in the plant TCA cycle. *Trends Plant Sci*. 2010:15:462–470. https://doi.org/10.1016/j.tplants.2010.05.006.

Sweetman C et al. AtNDB2 is the main external NADH dehydrogenase in mitochondria and is important for tolerance to environmental stress. *Plant Physiol*. 2019:181:774–788. https://doi.org/10.1104/pp.19.00877.

Tao J et al. RCD1 promotes salt stress tolerance in Arabidopsis by repressing ANAC017 activity. *Int J Mol Sci*. 2023:24:9793. https://doi.org/10.3390/ijms24129793.

Tiwari A et al. Differential FeS cluster photodamage plays a critical role in regulating excess electron flow through photosystem I. *Nat Plants*. 2024:10:1592–1603. https://doi.org/10.1038/s41477-024-01780-2.

Tran HC et al. An mTRAN-mRNA interaction mediates mitochondrial translation initiation in plants. *Science*. 2023:381:eadg0995. https://doi.org/10.1126/science.adg0995.

Triozzi PM et al. Spatiotemporal oxygen dynamics in young leaves reveal cyclic hypoxia in plants. *Mol Plant*. 2024:17:377–394. https://doi.org/10.1016/j.molp.2024.01.006.

Umbach AL, Fiorani F, Siedow JN. Characterization of transformed Arabidopsis with altered alternative oxidase levels and analysis of effects on reactive oxygen species in tissue. *Plant Physiol*. 2005:139:1806–1820. https://doi.org/10.1104/pp.105.070763.

Vainonen JP et al. Poly(ADP-ribose)-binding protein RCD1 is a plant PARylation reader regulated by photoregulatory protein kinases. *Commun Biol*. 2023:6:429. https://doi.org/10.1038/s42003-023-04794-2.

Van Aken O et al. Mitochondrial type-I prohibitins of Arabidopsis thaliana are required for supporting proficient meristem development. *Plant J*. 2007:52:850–864. https://doi.org/10.1111/j.1365-313X.2007.03276.x.

Van Aken O, Ford E, Lister R, Huang S, Millar AH. Retrograde signalling caused by heritable mitochondrial dysfunction is partially mediated by ANAC017 and improves plant performance. *Plant J*. 2016:88:542–558. https://doi.org/10.1111/tpj.13276.

van Dongen JT, Licausi F. Oxygen sensing and signaling. *Annu Rev Plant Biol*. 2015:66:345–367. https://doi.org/10.1146/annurev-arplant-043014-114813.

Vanlerberghe GC. Alternative oxidase: a mitochondrial respiratory pathway to maintain metabolic and signaling homeostasis during abiotic and biotic stress in plants. *Int J Mol Sci*. 2013:14:6805–6847. https://doi.org/10.3390/ijms14046805.

Vanlerberghe GC, Dahal K, Alber NA, Chadee A. Photosynthesis, respiration and growth: a carbon and energy balancing act for alternative oxidase. *Mitochondrion*. 2020:52:197–211. https://doi.org/10.1016/j.mito.2020.04.001.

van Veen H, Triozzi PM, Loreti E. Metabolic strategies in hypoxic plants. *Plant Physiol*. 2024:197:kiae564. https://doi.org/10.1093/plphys/kiae564.

Vaseghi M-J et al. The chloroplast 2-cysteine peroxiredoxin functions as thioredoxin oxidase in redox regulation of chloroplast metabolism. *eLife*. 2018:7:e38194. https://doi.org/10.7554/eLife.38194.

Vishwakarma A, Kumari A, Mur LAJ, Gupta KJ. A discrete role for alternative oxidase under hypoxia to increase nitric oxide and drive energy production. *Free Radic Biol Med*. 2018:122:40–51. https://doi.org/10.1016/j.freeradbiomed.2018.03.045.

Wagner S, Van Aken O, Elsässer M, Schwarzländer M. Mitochondrial energy signaling and its role in the low-oxygen stress response of plants. *Plant Physiol*. 2018:176:1156–1170. https://doi.org/10.1104/pp.17.01387.

Wang Y et al. Linking mitochondrial and chloroplast retrograde signalling in plants. *Philos Trans R Soc Lond B Biol Sci*. 2020:375:20190410. https://doi.org/10.1098/rstb.2019.0410.

Waszczak C, Carmody M, Kangasjärvi J. Reactive oxygen species in plant signaling. *Annu Rev Plant Biol*. 2018:69:209–236. https://doi.org/10.1146/annurev-arplant-042817-040322.

Weits DA, van Dongen JT, Licausi F. Molecular oxygen as a signaling component in plant development. *New Phytol*. 2021:229:24–35. https://doi.org/10.1111/nph.16424.

Wirthmueller L et al. Arabidopsis downy mildew effector HaRxL106 suppresses plant immunity by binding to RADICAL-INDUCED CELL DEATH1. *New Phytol*. 2018:220:232–248. https://doi.org/10.1111/nph.15277.

Xu S, Guerra D, Lee U, Vierling E. S-nitrosoglutathione reductases are low-copy number, cysteine-rich proteins in plants that control multiple developmental and defense responses in Arabidopsis. *Front Plant Sci*. 2013:4:430. https://doi.org/10.3389/fpls.2013.00430.

Yoshida K, Hara A, Sugiura K, Fukaya Y, Hisabori T. Thioredoxin-like2/2-Cys peroxiredoxin redox cascade supports oxidative thiol modulation in chloroplasts. *Proc Natl Acad Sci U S A*. 2018:115:E8296–E8304. https://doi.org/10.1073/pnas.1808284115.

Yoshida K, Noguchi K. Interaction between chloroplasts and mitochondria: activity, function, and regulation of the mitochondrial respiratory system during photosynthesis. In: Kempken F, editors. *Plant mitochondria. Advances in plant biology*. 2011:vol 1. Springer; 2011. p. 383–409. https://doi.org/10.1007/978-0-387-89781-3_15.

Zhang R et al. A high-resolution single-molecule sequencing-based Arabidopsis transcriptome using novel methods of Iso-seq analysis. *Genome Biol*. 2022:23:149. https://doi.org/10.1186/s13059-022-02711-0.